Neural Comput & Applic (2017) 28 (Suppl 1):S707–S718
DOI 10.1007/s00521-016-2368-7

ORIGINAL ARTICLE

Prediction of properties of self-compacting concrete containing fly ash using artificial neural network

Omar Belalia Douma[1] · Bakhta Boukhatem[1] · Mohamed Ghrici[1] · Arezki Tagnit-Hamou[2]

Received: 22 December 2014 / Accepted: 21 May 2016 / Published online: 7 June 2016

Abstract This paper investigates the feasibility of using artificial neural networks (ANNs) modeling to predict the properties of self-compacting concrete (SCC) containing fly ash as cement replacement. For the purpose of constructing this model, a database of experimental data was gathered from the literature and used for training and testing the model. The data used in the artificial neural network model are arranged in a format of six input parameters that cover the total binder content, fly ash replacement percentage, water–binder ratio, fine aggregates, coarse aggregates and superplasticizer. Four outputs parameters are predicted based on the ANN technique as the slump flow, the L-box ratio, the V-funnel time and the compressive strength at 28 days of SCC. To demonstrate the utility of the proposed model and improve its performance, a comparison of the ANN-based prediction model with other researcher's experimental results was carried out, and a good agreement was found. A sensitivity analysis was also conducted using the trained and tested ANN model to investigate the effect of fly ash on SCC properties. This study shows that artificial neural network has strong potential as a feasible tool for predicting accurately the properties of SCC containing fly ash.

Keywords Self-compacting concrete · Fly ash · Prediction · Neural network · Rheological properties · Compressive strength

✉ Omar Belalia Douma
bel_dou@hotmail.fr

[1] Geomaterials Laboratory, Department of Civil Engineering, Faculty of Civil Engineering and Architecture, University of Chlef, BP 151, 02000 Chlef, Algeria

[2] Department of Civil Engineering, University of Sherbrooke, Sherbrooke, QC, Canada

1 Introduction

Concrete is one of the most widely used construction materials in the world. However, much of the current available knowledge on concrete technology has been mainly generated in the most developed parts of the world [1]. During the last years, special types of concrete like high-performance concrete and self-compacting concrete are commonly used.

Self-compacting concrete (SCC) has emerged in Japan in the late 1980s as a material that can flow under its own weight. This allows the facility of concrete placement without the need of additional mechanical compaction in complicated formwork, congested reinforced structural elements and hard to reach areas [2, 3]. This saves time, reduces overall cost, improves working environment and opens the way for the automation of the concrete construction. SCC is an innovative homogeneous and dense concrete in hardened state, and it has the same engineering properties and durability as traditional vibrated concrete.

Many researchers have set some guidelines for mixture proportioning of SCC, which include reducing the volume ratio of aggregate to cementitious material; increasing the paste volume and water–cement ratio (w/c); carefully controlling the maximum coarse aggregate particle size and total volume; and using various viscosity enhancing admixtures [4]. For SCC, it is generally necessary to use superplasticizers in order to obtain high workability and viscosity-modifying admixture eliminate segregation. Adding chemical admixtures are, however, expensive, and their use may increase the materials cost. Savings in labor cost might offset the increased cost, but the use of mineral additions could increase the slump of the concrete mixture without increasing its cost. These new building materials are known as supplementary cementing materials (SCMs) that are defined as material from the waste stream of a manufacturing process. These include fly ash, silica fume and blast furnace slag or limestone filler. Their use as a partial replacement for Portland cement reduces the amount of cement needed for concrete. This reduces the energy and CO_2 impacts of concrete and helps improve the workability and long-term properties of concrete [5].

Fly ash (FA) is the finely divided residue that results from the combustion of ground or powdered coal and that is transported by flue gases from the combustion zone to the particle removal system [6]. Fly ash is an industrial by-product and is considered one of the most widely used in different concrete applications. When FA is used as a mineral admixture in concrete, it improves its strength and durability characteristics at later ages depending on its reactivity, the distribution of particle size and the carbon content. Generally, FA is used as a partial replacement of cement. However, it can also be used as a partial replacement of fine aggregates to achieve different concrete properties. Previous investigations show that the use of FA in SCC reduces the dosage of superplasticizer needed to obtain similar slump flow compared to concrete made with Portland cement only [7]. In addition, the use of FA improves significantly the rheological properties and reduces concrete cracking due to the heat of hydration of cement [8].

A few studies have been carried out on the optimization of the mix proportion by the addition of FA to SCC. It is reported that 30 % of cement replacement optimized percentage of FA in SCC resulted in excellent workability and flowability [9]. However, due to difference in quality and quantity of material constituents and depending on the adopted design specifications, an uncertainty is created in establishing a general relationship between FA and cement ratio, chemical admixtures and w/c ratio. Meanwhile, there is insufficient research on modeling the rheological and mechanical properties of SCC with FA where the most of the researches are based on traditional methods.

For the last two decades, different modeling methods based on artificial intelligence (AI) techniques have become popular like artificial neural networks (ANNs), fuzzy logic (FL) systems, genetic algorithm (GA) and expert system (ES). Those methods have been used by many researchers for a variety of engineering applications [10]. In civil engineering, many researchers proposed models using these techniques for predicting concrete properties [11–13]. For SCC, these techniques are also used by some researchers proposing many predictive models. A fuzzy logic prediction model for fresh and hardened properties of SCC containing fly ash and polypropylene fibers was developed by Gencel et al. [14]. A shrinkage prediction models for SCC based on an independent methodology that combines fuzzy logic and genetic algorithm were developed by Da Silva and Štemberk [15]. An expert system was developed with the goal of classifying the surface finish of SCC precast elements by Da Silva and Štemberk [16]. A fuzzy inference system was built for the specific case of various SCC mixtures subjected to ammonium sulfate attack by Nehdi and Bassuoni [17].

ANNs are based on the principle that a highly interconnected system of simple processing elements can learn the nature of complex interrelationships between independent and dependent variables. Artificial neural networks are one of the most widely used methods for predicting SCC properties. Several investigations were carried out to develop ANN models for predicting rheological and mechanical properties of SCC. Some researchers focused on predicting the SCC compressive strength [18–20], while others used some rheological properties of SCC like setting times and slump flow [21, 22]. The prediction of the SCC performance with fly ash was initially tried using a neural network with single architecture [23, 24].

However, all the previous proposed ANN models for predicting each property separately, none of them considered both of the most important rheological and mechanical properties.

In this context, the main purpose of this study is to develop an ANN model for predicting the most important rheological properties combined with the most important mechanical property (the compressive strength at 28 days) based on mixture proportioning of SCC with fly ash, while maintain the same architecture. The slump flow test, V-funnel time test and the L-box test are used to evaluate the flowability, viscosity, filling ability and the passing ability.

2 Artificial neural networks (ANNs)-based model

Artificial neural networks (ANNs) are computing systems that simulate the biological neural systems of the human brain exhibiting the ability to learn reason and solve problems [25]. They are a family of massively parallel architectures that can be used to solve difficult problems described by a large amount of data via the cooperation of highly interconnected but simple computing elements (Fig. 1). These units are commonly referred to as neurons. Each neuron receives an input signal from the neurons to which it is connected. Each of these connections has numerical weights associated with them. These weights determine the nature and strength of the influence between the interconnected neurons. The signals from each input are then processed through a weighted sum on the inputs. The processed output signal is then transmitted to another neuron via a transfer function. The transfer function adjusts the weighted sum of the inputs so that the output approaches unity when the input gets larger and approaches zero when the input gets smaller.

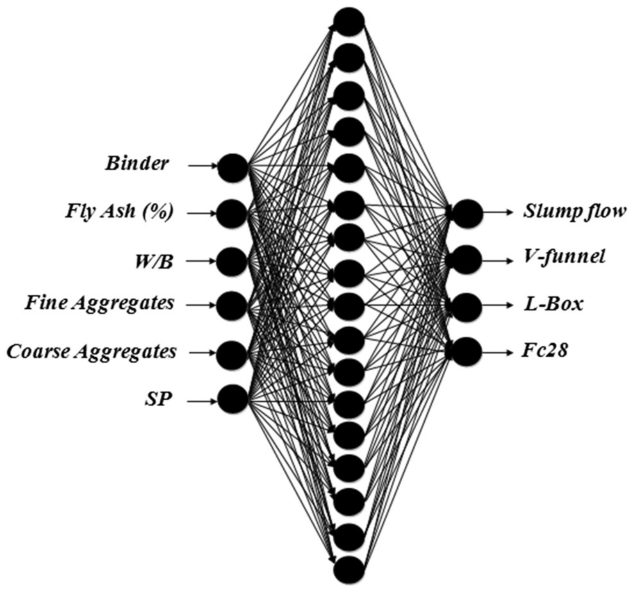

Fig. 1 Architecture used in the neural network model

Back-propagation is generally known to be the most powerful and widely used supervised learning technique to train a network [26]. To obtain some desired outputs, weights, which represent connection strength between neurons and biases, are adjusted using a number of training inputs and the corresponding target values. The network error, that is the difference between calculated and expected target patterns, is then back-propagated from the output layer to the input layer to update the network weights and biases. The input and output neurons are defined by the problem to be solved, whereas the number of hidden layers and the corresponding number of neurons per layer may be determined by trialing different configurations until reaching the optimum. The network errors that arise during the learning process can be expressed in terms of mean square error (MSE) and are calculated using Eq. (1).

$$\mathrm{MSE} = \left(\frac{1}{p}\right) * \sum_{j} \left(t_j - o_j\right)^2 \tag{1}$$

In addition, the absolute fraction of variance (R^2) and mean absolute percentage error (MAPE) are calculated using Eqs. (2) and (3), respectively.

$$R^2 = 1 - \left(\frac{\sum_j \left(t_j - o_j\right)^2}{\sum_j \left(o_j\right)^2}\right) \tag{2}$$

$$\mathrm{MAPE} = \frac{1}{p}\sum_j \left(\left|\frac{o_j - t_j}{o_j}\right| * 100\right) \tag{3}$$

where t_j is the target value of jth pattern, O_j is the output value of jth pattern and P is the number of patterns.

2.1 Data collection

The main purpose of this study is to develop an ANN model to predict rheological and mechanical properties of self-compacting concrete with fly ash. In most previous research, all applications predict one property of concrete through a large number of components. The primary goal in this model is to predict a large number of outputs from a limited number of inputs, the more we can predicted a number of properties of SCC from a limited number of its components as much as possible, the model will be successful and applicable in the field. Sufficient data are collected to build a database consisting a set of data on fly ash SCC mixtures. The data were obtained from different sources and used for training and testing the ANN model. To construct this model, a total number of 114 different experimental data were gathered from the literature (see Appendix for table showing the data source collected for constructing the model) [27–39].

The data used in the proposed neural networks model are arranged in a format of six input parameters that cover the binder content, fly ash percentage, water–binder ratio, fine aggregates, coarse aggregates and superplasticizer. The majority of previous works construct a database from their experimental results, so the results are limited just for their environment, but our database is built from many different sources of data including the literature in different countries; moreover, it can be applied in a wider area. Four outputs parameters are predicted by the ANN model as the slump flow diameter, the L-box ratio, the V-funnel time and the compressive strength at 28 days of SCC. The boundary values for input and output variables used in the multilayer feed-forward neural network model are listed in Table 1. The input parameters are distributed in different ranges in a homogeneous form for training the model as shown in Table 2.

Table 1 Input and output quantities

Components	Minimum	Maximum	Average
Input variables			
Binder (kg/m^3)	370.00	733	523.4
Water/binder	0.26	0.45	0.37
Fly ash (%)	0.00	60	28.7
Fine aggregates (kg/m^3)	656	1038	852.8
Coarse aggregates (kg/m^3)	590	935	742.63
Superplastisizer (kg/m^3)	0.74	21.84	8
Output variables			
D flow (mm)	480	880	660.5
L-box (H_2/H_1)	0.6	1	0.86
V-funnel (s)	1.95	19.2	7.75
Compressive strength (MPa)	10.2	86.8	48.22

Table 2 Distribution of inputs in the data base

Binder		Water/binder		Fly ash		Coarse aggregates		Fine aggregates		Superplastisizer	
Rang (kg/m^3)	Freq	Rang	Freq	Rang (%)	Freq	Rang (kg/m^3)	Freq	Rang (kg/m^3)	Freq	Rang (kg/m^3)	Freq
350–450	24	0.25–0.30	19	0–15	23	650–750	19	600–700	48	0–5	33
451–550	69	0.31–0.35	30	16–30	45	751–850	29	701–800	19	6–10	51
551–650	18	0.36–0.40	17	31–45	29	851–950	55	801–900	42	11–15	19
651–750	3	0.41–0.45	48	46–60	17	951–1050	11	901–1000	5	16–20	11

2.2 Training the ANN model

For building and training the neural network model, specialized computer software was used [40]. A MATLAB-based program with a graphical user interface (GUI) was developed to train and test the ANN model. To provide an ANN model with good generalization capability, the data were divided into sets: (91) training and (23) testing patterns (randomly selected 20 % of data as testing set).To avoid over-fitting (over-training), thus enabling a good generalization capability, 11 validation patterns were used to stop earlier the training process.

A multilayer perceptron (MLP) was employed in this research of three layers: an input layer, a hidden layer and an output layer. Each layer consists of a number of neurons. The neurons of the input layer receive information from the outside environment and transmit them to the neurons of the hidden layers without performing any calculations. The hidden layer neurons then process the incoming information and extract useful features to reconstruct the mapping from the input space. The neighboring layers are fully interconnected by weights. Finally, the output layer neurons produce the network predictions to the outside world. There is no general rule for selecting the number of neurons in a hidden layer. The choice of hidden layer size is mainly a problem and to some extent depends on the number and quality of the training pattern. The numbers of neurons in input and output layers are based on the geometry of the problem. Nevertheless, there is no general rule for selection of the number of neurons in a hidden layer. Hence, they are determined by trial-and-error method in this study. It should be noted that it is possible to achieve satisfactory results with different network architectures. This involved the development and testing more than 1000 architectures with various numbers of hidden layers and neurons in hidden layer sizing the back-propagation algorithm. Consequently, the ANN model was selected as having 6 neurons in input layer representing influential parameters (binder content, percentage replacement of fly ash, water-to-binder ratio, fine aggregates, coarse aggregates and superplasticizer), 17 neurons in hidden layer and 4 neurons in output layer (slump flow, V-funnel, L-box ratio, compressive strength at 28 days) as illustrated in Fig. 1.

Table 3 Parameters used in the neural network model

Parameters	ANN
Number of input layer neurons	6
Number of hidden layer	1
Number of first hidden layer neurons	17
Number of output layer neuron	4
Momentum rate	0.9
Learning rate	0.5
Learning cycle	11

A tangent sigmoid transfer function was employed as an activation function for all neurons. Weights and biases were randomly initialized. A maximum number of epochs (learning cycles) reached during the training of the network model was 1000. The following values of network training parameters are summarized in Table 3.

Accordingly, a comparison between experimental values and those predicted by the ANN showed a high correlation proving its high accuracy in estimating target value in the training phase as well as in the validation and the testing phase (Fig. 2).

2.3 Validation of ANN model

The validity of a successfully trained ANN model is determined by its ability to generalize its predictions beyond the training data and to perform well when it is presented with unfamiliar new data within the range of the input parameters used in the training. Therefore, the ability of the proposed ANN model developed to predict the SCC properties of new data obtained by additional results from other researcher's excluded from the training data must be validated. The more data available, the more reliable a prediction of SCC properties by ANN will be obtained.

The model was presented with a total of 16 unseen records and was required to predict the four SCC properties associated with each set of values within the six influential parameters [41–44]. The comparison between the predicted values by the developed ANN model and the validation new data records is shown in Table 4. In this table, the

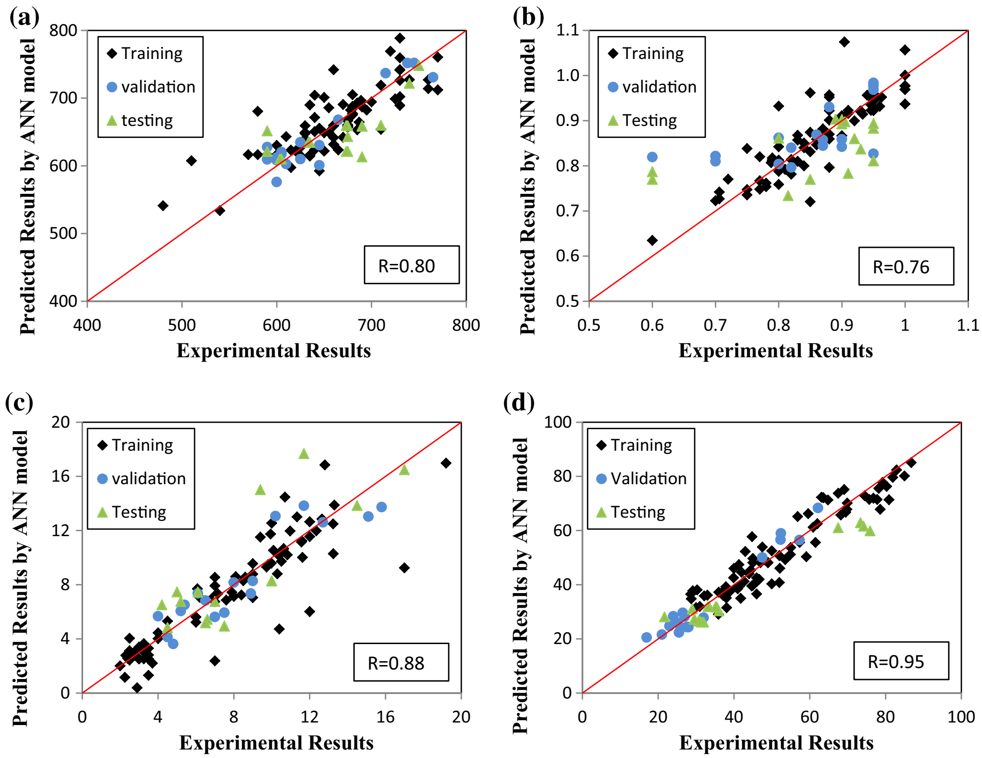

Fig. 2 Linear relationship between experimental and predicted properties for SCC. **a** Slump flow (mm), **b**, L-box ratio, **c** V-funnel time (s) and **d** compressive strength (MPa)

computed relative error in each prediction as expressed by Eq. 4 is represented correctly.

$$E(\%) = \mathrm{ABS}\left(\frac{O_{\mathrm{exp}} - O_{\mathrm{ANN}}}{O_{\mathrm{exp}}}\right) * 100 \quad (4)$$

where O_{exp} is the experiment output and O_{ANN} is the output obtained by the ANN model.

The validation of the ANN model is represented in a total relative error, and it indicates that using the proposed model is possible to accurately predict the slump flow value, the V-funnel time, the L-box ratio and the compressive strength at 28 days of SCC containing different percentages of fly ash.

3 Parametric analysis based on ANN model results

Because of the complexity of the system, it is difficult to identify the change on different output parameters on this model by the change of just one parameter. However, in order to check the capability of the ANN model to capture the sensitivity of SCC mix properties to individual constituents, a parametric analysis was carried out.

3.1 Effect of fly ash content

The simulation results of various fresh properties as slump flow diameter; L-box test [ratio of heights at the two edges of L-box (H_2/H_1)]; V-funnel test (time taken by concrete to flow through V-funnel); and the compressive strength at 28 days with fly ash replacement level (from 0 to 60 %) at various binder contents (350, 450 and 550 kg/m^3) are shown in Fig. 3. In this case, a great effect of replacement level of fly ash on the outputs parameters was found. Test results of this analysis indicated that all SCC mixes meet the requirements of allowable slump flow, L-box, V-funnel flow time and compressive strength. This improves concrete performance in both the fresh and hardened state.

The slump flow diameter improves with the increase in fly ash content and decreases with the increase in binder content at any level of fly ash (Fig. 3a). This produces a paste with improved plasticity and more cohesiveness. All the values of the predicted slump flow obtained by the ANN model for all binder content in this analysis are in the range of 640–790 mm which maintains the workability of SCC mixes within the acceptable slump flow range (500–800 mm) [4].

The L-box passing ability of the SCC mixtures with fly ash increased with the increase in fly ash replacement level. All the L-box ratio values converge to some point within 0.7–0.9 at 30 % of fly ash replacement (Fig. 3b). It was also observed that as the replacement percentages of fly ash continue to increase up to 30 %, the L-box ratio was in the range of 0.8–1, the generally recommended values [4].

The V-funnel passing time get reduces as the fly ash percentage increases (Fig. 3c). In this study, the V-funnel

Table 4 Comparison of ANN-based model with other researcher's results

N	Author	year	FA (%)	D (mm)			L-Box (H_2/H_1)			V-funnel(s)			Fc 28 (MPa)		
				Exp	ANN	E (%)	Exp	ANN	E (%)	Exp	ANN	E (%)	Exp	ANN	E (%)
1	Zhu [41]	2003	0	600	594	1.0							66.8	61.78	7.5
2			20	600	610	1.7							71.3	66.36	6.9
3			30	630	612	2.8							49.9	53.4	7.0
4	Naik [42]	2012	0	679	734	8.0							60	75.82	26.4
5			35	686	690	0.5							62	62.9	1.5
6			45	686	638	6.9							60	66.48	10.8
7			55	699	631	9.8							48	60.74	26.5
8	Turk [43]	2013	0	709	651	8.1	0.89	0.84	5.7				57.5	77.13	34.1
9			25	709	621	12.4	0.91	0.74	18.8				53.5	55.26	3.3
10			30	702	640	8.8	0.94	0.77	17.9				55	56.72	3.1
11			35	705	657	6.7	0.95	0.8	15.6				58	57.19	1.4
12			40	701	676	3.5	0.96	0.84	12.7				59	57.81	2.0
13	Liu [44]	2010	0	720	652	9.4				8.1	5.7	29.4	73.3	63.06	14.0
14			20	700	670	4.3				8.1	4.5	44.7	69.7	51.79	25.7
15			40	705	709	0.6				6.1	4.7	22.4	58.5	42.42	27.5
16			60	715	745	4.2				6.3	3.1	50..2	37.2	36.18	2.8

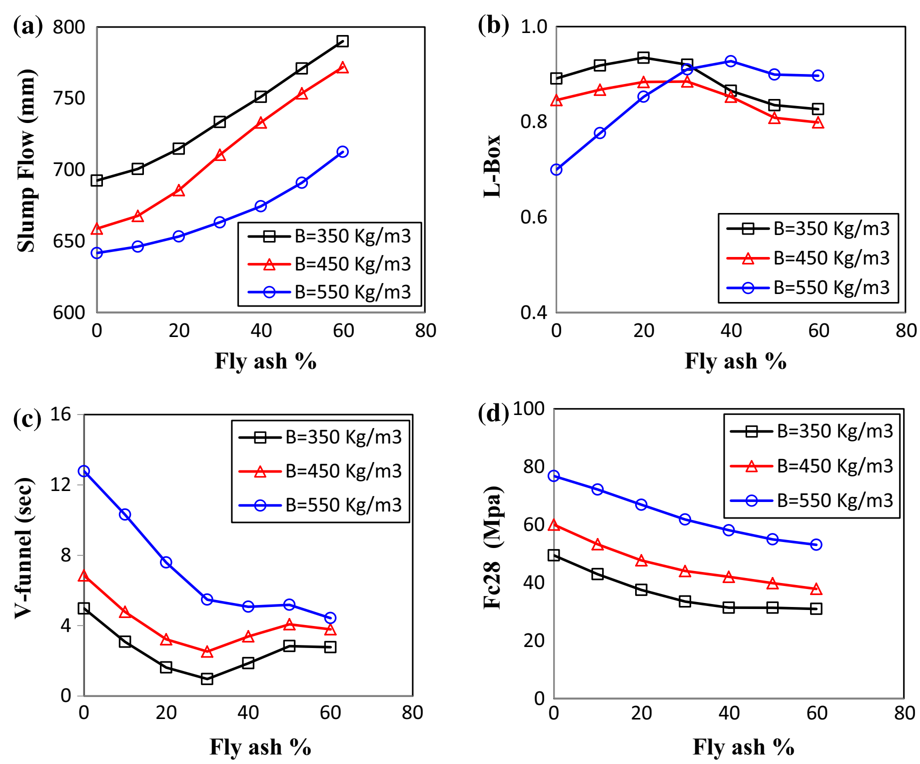

Fig. 3 Effect of fly ash on properties of SCC. **a** Slump flow (mm), **b** L-box ratio, **c** V-funnel time (s) and **d** compressive strength at 28 days (MPa)

flow times predicted values were in the range of 4–13 s, which confirm the adequate V-funnel time for the SCC (<27 s).

The compressive strength at 28 days is found to decrease with the increase in fly ash content and to increase with increasing the binder content (Fig. 3d). This strongly influenced the SCC strength with constant water-to-binder ratio. The decrease in the compressive strength is directly dependent on the amount of cement replacement by the fly ash which agrees with previously published results [42].

3.2 Effect of water–binder ratio

The variation of the slump flow, V-funnel time, L-box ratio and the compressive strength at 28 days with water-to-binder ratio (w/b) for different quantities of fly ash is shown in Fig. 4.

The slump flow diameter values increases with the increase in water–binder ratio and fly ash content (Fig. 4a). It has been also shown that fly ash has the highest potential to be used in SCC. This was especially the case for producing highly workable SCC with high volume of the paste mortar, which often leads to a higher water-to-binder ratio [5].

All the L-box ratio values converge to some point within 0.75–0.95 and increase with increasing the fly ash content for water–binder ratio up to 0.37 (Fig. 4b). This was inverted when using lower percentage of fly ash and water–binder ratio.

The V-funnel passing time get reduce as the fly ash percentage increases from 20 to 60 % (Fig. 4c). Almost the V-funnel time values, which are <6 s, are recommended for concrete to qualify as a SCC.

The combined influences of an increase in fly ash content from 20 to 60 % and water–binder ratio from 0.30 to 0.45 decrease the 28-day compressive strength of SCC (Fig. 4d). This agrees well with previously published results [37].

3.3 Effect of Superplasticizer

Superplasticizer plays a fundamental role to improve the rheological properties of SCC. It is an essential material component that must be used to produce SCC. The variation of the slump flow, V-funnel time, L-box ratio and the compressive strength at 28 days with superplasticizer dosages (from 1 % to 4 %) for different quantities of fly ash is shown in Fig. 5.

The slump flow diameter and the L-box ratio are increased with increasing the superplastisizer dosages up to 1 % and fly ash content (Fig. 5a, b). The slump flow seems to be related to the dosage of superplasticizer. The V-funnel flow time decreases with increasing both of the superplastisizer and the fly ash dosages (Fig. 5c). Those results are consistent with the results of other researchers which showed that the superplasticizer improves the flowability of SCC by their liquefying and dispersing actions [45].

The compressive strength at 28 day is seen to decrease with the increase in fly ash content and superplastisizer dosages until it reaches a specific value so that the effect does not appear significantly (Fig. 5d). The superplastisizer can either increase the strength by lowering the quantity of mixing water for a given flowability or reduce both cement and water contents to achieve a given strength and flowability [46]. At given water-to-binder ratio, the use of fly ash

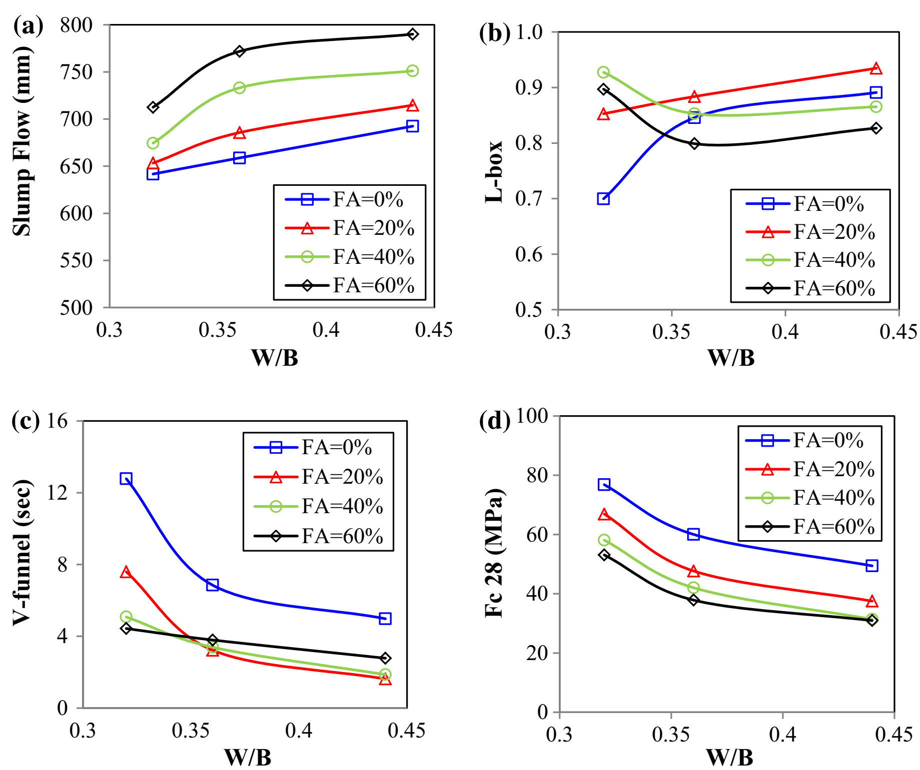

Fig. 4 Effect of water–binder ratio on properties of SCC. **a** Slump flow (mm), **b** L-box ratio, **c** V-funnel time (s) and **d** compressive strength at 28 days (MPa)

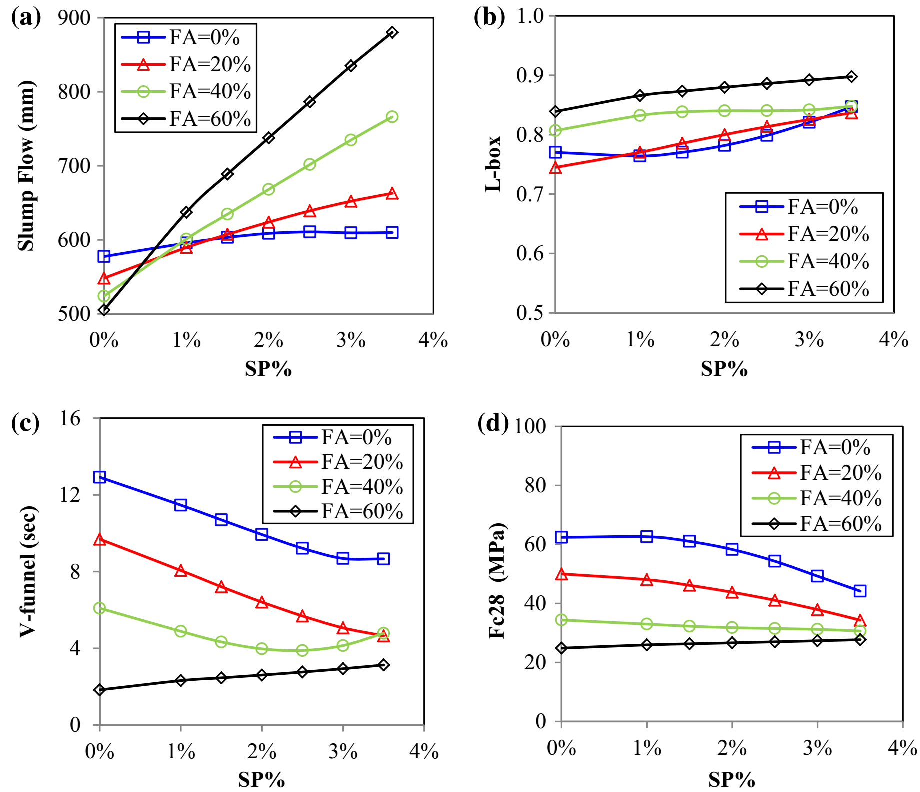

Fig. 5 Effect of superplasticizer on properties of SCC. **a** Slump flow (mm), **b** L-box ratio, **c** V-funnel time (s) and **d** compressive strength at 28 days (MPa)

in SCC reduces the dosage of superplasticizer needed to obtain similar strength compared to SCC made with Portland cement only [42].

In fact, it is difficult to simplify the interaction of the superplasticizer on SCC mix properties. In addition, there is a correlation between the superplasticizer adsorption on the particles surface, which depend on many parameters (the charge density of the polymers, the zeta potential, pore solution ionic content and strength, cement and cement blending materials chemistry).

4 Conclusion

In this study, artificial neural network is used for predicting different properties of SCC containing volume of fly ash as a cement replacement. For this purpose, a feed-forward neural network comprising of one hidden layer with 17 neurons and a back-propagation training algorithm was used. The study conducted and presented in this paper shows the feasibility of using a simple ANN to predict both rheological and mechanical properties of SCC. It was demonstrated that the developed ANN model was successfully trained and validated. SCC is a complex material, and there is correlation between many factors. ANNs is a highly interconnected system that can learn the nature of complex interrelationships between independent and dependent variables. As a result, the model was able to predict the slump flow, L-box ratio, V-funnel time and compressive strength at 28 days. It was mentioned the capability of model to recognize and evaluate the effect of individual constituents that cover the total binder content, fly ash replacement percentage, water–binder ratio, fine aggregates, coarse aggregates and superplasticizer on the properties of SCC.

Appendix: Data sources

See Table 5.

Author	Year	B	P	W/B	F	C	SP	D (mm)	L_{box}	V_{funnel}	Fc28
Gettu et al. [29]	2002	701	37	0.27	774	723	8.10	580	0.80	10.0	69.5
		733	37	0.26	748	698	8.40	660	0.90	12.0	68.2
Patel [35]	2003	400	30	0.39	946	900	1.40	510	0.96	4.5	45.0
		370	36	0.43	960	900	1.85	650	0.94	3.0	46.0
		430	36	0.43	830	900	0.86	480	0.60	2.5	36.0
		430	36	0.43	827	900	2.15	810	0.95	2.0	48.0
		400	45	0.45	850	900	1.40	760	1.00	2.5	38.0
		400	45	0.39	916	900	1.40	580	1.00	3.0	45.0
		400	45	0.39	916	900	1.40	600	1.00	3.0	47.0
		400	45	0.39	916	900	1.40	570	1.00	3.0	49.0
		400	45	0.39	916	900	1.40	590	1.00	3.3	49.0
		400	45	0.39	916	900	1.40	590	1.00	3.5	49.0
		400	45	0.39	916	900	2.40	770	1.00	3.5	43.0
		450	45	0.39	808	900	1.58	680	1.00	2.3	50.0
		370	54	0.43	930	900	0.74	600	1.00	2.8	31.0
		370	54	0.43	928	900	1.85	760	1.00	2.5	33.0
		430	54	0.34	874	900	0.86	540	0.87	3.3	46.0
		430	54	0.36	872	900	2.15	710	1.00	4.0	52.0
		400	60	0.39	886	900	1.40	630	0.91	3.5	44.0
Sahmaran et al. [36]	2009	500	0	0.35	1038	639	6.75	665	0.87	12.7	62.2
		500	30	0.34	1006	620	6.75	765	0.95	10.2	52.4
		500	30	0.35	1008	621	6.75	715	0.95	15.8	57.3
		500	40	0.35	995	613	6.75	730	0.85	10.7	59.1
		500	40	0.32	1004	618	6.75	745	0.95	11.7	52.3
		500	50	0.35	988	608	6.75	710	0.90	19.2	40.8
		500	50	0.3	1010	628	6.75	738	0.88	15.1	47.5
		500	60	0.35	979	603	6.75	740	0.85	12.8	38.1
		500	60	0.3	997	614	6.75	770	0.95	9.4	39.9
Güneyisi et al. [30]	2010	550	0	0.44	826	868	3.50	670	0.71	3.2	61.5
		550	0	0.32	728	935	8.43	670	0.79	17.0	80.9
		550	20	0.44	813	855	3.20	675	0.71	10.4	52.1
		550	20	0.32	714	917	7.43	730	0.93	7.0	69.8
		550	40	0.44	801	842	2.96	730	0.80	6.0	44.7
		550	40	0.32	700	899	7.43	730	0.96	6.0	60.9
		550	60	0.44	788	829	3.00	720	0.95	4.0	30.3
		550	60	0.32	686	881	6.67	730	0.90	7.0	47.5
Mahalingam and Nagamani [32]	2011	450	30	0.43	789	926	2.77	660	0.88	3.5	44.8
		500	30	0.39	731	862	6.15	640	0.75	2.5	53.6
		550	30	0.35	711	835	4.74	610	0.86	3.2	57.3
		450	40	0.43	780	917	2.77	650	0.88	3.7	41.3
		500	40	0.39	724	850	6.15	680	0.88	2.3	46.7
		550	40	0.35	701	823	6.77	730	0.90	3.4	54.9
		450	50	0.43	770	907	2.50	675	0.72	2.7	37.1
		500	50	0.39	714	836	4.92	730	0.88	2.9	41.8
		550	50	0.35	703	824	5.41	725	0.88	2.4	44.4

continued

Author	Year	B	*P*	W/B	F	C	SP	D (mm)	L_{box}	V_{funnel}	Fc28
Siddique et al. [38]	2011	550	15	0.41	910	590	10.73	673	0.89	7.5	35.2
		550	20	0.41	910	590	11.01	690	0.95	4.5	33.2
		550	25	0.42	910	590	9.91	603	0.85	5.2	31.5
		550	30	0.43	910	590	9.91	673	0.95	6.1	30.7
		550	35	0.44	910	590	9.91	633	0.92	10.0	29.6
Uysal and Yilmaz [39]	2011	550	0	0.33	869	778	8.80	690	0.82	14.5	75.9
		550	15	0.33	865	762	8.80	710	0.91	9.4	74.2
		550	25	0.33	887	752	8.80	740	0.93	11.7	73.4
		550	35	0.33	878	742	8.80	750	0.91	17.0	67.5
Seddique [37]	2012	550	15	0.41	910	590	9.90	625	0.82	4.0	26.5
		550	15	0.41	910	590	10.17	675	0.80	6.6	36.0
		550	15	0.41	910	590	10.45	590	0.95	6.5	29.0
		550	15	0.41	910	590	10.72	675	0.90	7.5	35.5
		550	20	0.41	910	590	6.60	600	0.70	4.8	24.0
		550	20	0.41	910	590	7.15	645	0.95	4.5	27.0
		550	20	0.41	910	590	9.90	605	0.82	7.5	32.0
		550	20	0.41	910	590	11.00	690	0.90	4.5	33.5
		550	25	0.42	910	590	7.70	600	0.60	7.0	26.0
		550	25	0.42	910	590	8.25	625	0.80	5.2	28.0
		550	25	0.42	910	590	9.90	605	0.60	7.0	32.0
		550	25	0.42	910	590	11.00	590	0.60	4.2	21.7
		550	30	0.43	910	590	7.15	610	0.87	5.4	21.0
		550	30	0.43	910	590	7.70	600	0.90	6.5	25.5
		550	30	0.43	910	590	8.80	605	0.70	8.9	27.5
		550	30	0.43	910	590	9.90	675	0.95	5.0	31.0
		550	35	0.44	910	590	7.15	590	0.86	6.1	17.0
		550	35	0.44	910	590	8.80	590	0.80	8.0	23.0
		550	35	0.44	910	590	9.35	645	0.90	9.0	25.0
		550	35	0.44	910	590	9.90	635	0.92	10.0	29.5
Muthupriya et al. [33]	2012	500	30	0.35	900	600	11.00	660	0.90	9.0	29.2
		500	40	0.35	900	600	10.75	675	0.93	7.0	28.6
		500	50	0.35	900	600	10.50	680	0.95	7.2	28.7
Dhiyaneshwaran et al. [27]	2013	530	0	0.45	768	668	4.55	660	0.92	12.0	30.0
		530	10	0.45	768	668	4.55	675	0.93	10.6	32.2
		530	20	0.45	768	668	4.55	680	0.95	9.8	37.9
		530	30	0.45	768	668	4.55	690	0.95	8.5	41.4
		530	40	0.45	768	668	4.55	685	0.95	7.9	37.2
		530	50	0.45	768	668	4.55	678	0.95	7.6	35.9
Bingöl and Tohumcu [28]	2013	500	0	0.35	967	694	8.00	630	0.84	6.1	78.6
		500	25	0.35	938	673	7.50	660	0.85	7.0	62.0
		500	40	0.35	923	663	7.50	680	0.88	6.2	55.0
		500	55	0.35	908	652	7.50	700	0.91	7.0	42.7
Krishnapal et al. [31]	2013	450	0	0.45	890	810	9.25	687	0.80	9.0	50.0
		480	0	0.4	890	810	13.30	650	0.88	12.0	52.0
		450	10	0.45	890	810	8.20	689	0.79	8.6	45.0
		480	10	0.4	890	810	9.90	665	0.85	9.0	46.0
		450	20	0.45	890	810	6.40	690	0.78	8.0	41.0
		480	20	0.4	890	810	9.68	685	0.82	8.4	42.0
		450	30	0.45	890	810	4.80	695	0.78	8.0	39.0
		480	30	0.4	890	810	9.40	680	0.80	8.1	40.0

continued

Author	Year	B	*P*	W/B	F	C	SP	D (mm)	L_{box}	V_{funnel}	Fc28
Nepomuceno et al. [34]	2014	575	0	0.31	794	772	17.22	645	0.75	13.3	77.8
		589	0	0.31	813	729	17.64	640	0.75	10.6	76.8
		628	0	0.29	744	772	19.53	615	0.77	11.6	82.9
		633	0	0.27	656	875	20.58	635	0.79	13.2	86.8
		643	0	0.29	761	729	19.95	630	0.86	9.9	81.9
		670	0	0.27	695	772	21.84	620	0.81	10.4	85.0
		551	16	0.31	822	772	11.34	625	0.70	11.6	59.6
		564	16	0.31	841	729	11.55	630	0.77	10.3	56.8
		588	16	0.28	752	820	12.39	635	0.77	11.0	64.8
		604	16	0.28	772	772	12.71	625	0.80	9.7	63.1
		613	16	0.26	686	875	12.92	615	0.77	12.7	67.5
		618	16	0.28	790	729	13.02	640	0.83	11.6	63.6
		649	16	0.26	726	772	13.65	650	0.84	10.0	69.1
		613	24	0.26	685	875	15.33	645	0.80	13.3	78.2
		633	24	0.26	706	820	15.86	630	0.79	12.4	79.2
		649	24	0.26	726	772	16.28	655	0.84	10.5	80.3
		567	25	0.3	846	729	13.86	655	0.82	11.3	69.9
		607	25	0.27	774	772	15.12	640	0.83	10.8	74.5
		620	25	0.27	792	729	15.54	635	0.83	10.1	75.7

References

1. Zongjin L (2011) Advanced concrete technology. Wiley, Hoboken
2. Ozawa K, Maekawa K, Kunishima H, Okamura H (1989) Performance of concrete based on the durability design of concrete structures. Proc Second East Asia Pacific Conf Struct Eng Constr 1:445–456
3. Okamura H et al (1995) Self-compacting high performance concrete. Proc Fifth EA SEC 3:2381–2388
4. EFNARC (2005) Specification and guidelines for self-compacting concrete. EFNARC Association House, Hampshire
5. Neville AM (2005) Properties of concrete, 4th edn. Pearson Education Limited, Essex, England
6. Wesche K (2005) Fly ash in concrete properties and performance. Rilem Repport 7:2005
7. Yahia A, Tanimura M, Shimabukuro A, Shimovama Y (1999) Effect of rheological parameters on self-compactability of concrete containing various mineral admixtures. In: International RILEM symposium on self-compacting concrete, pp 523–535
8. Kurita M, Nomura T (1998) Highly-flowable steel fiber-reinforced concrete containing fly ash. In: Malhotra VM (ed) Proceedings of the sixth CANMET/ACI international conference on fly ash, silica fume, slag, and natural pozzolans in concrete, vol 178. ACI Special Publication, pp 159–175
9. Miura N, Takeda N, Chikamatsu R, Sogo S (1993) Application of super workable concrete to reinforced concreted structures with difficult construction conditions. In: Zia P (ed) High performance concrete in severe environments. ACI Special Publication, USA, pp 163–186
10. Boukhatem B, Kenai S, Tagnit-Hamou A, Ghrici M (2011) Application of new information technology on concrete: an overview. J Civ Eng Manag 17(2):248–258
11. Boukhatem B, Ghrici M, Kenai S, Tagnit-Hamou A (2011) Prediction of efficiency factor of ground-granulated blast-furnace slag of concrete using artificial neural network. ACI Mater J V 108(1):55
12. Başyigit C, Akkurt I, Kilincarslan S, Beycioglu A (2010) Prediction of compressive strength of heavyweight concrete by ANN and FL models. Neural Comput Appl 19(4):507–513
13. Severcan MH (2012) Prediction of splitting tensile strength from the compressive strength of concrete using GEP. Neural Comput Appl 21:1937–1945
14. Gencel O, Ozel C, Koksal F, Martinez-Barrera G, Brostow W, Polat H (2013) Fuzzy logic model for prediction of properties of fiber reinforced self-compacting concrete. Mater Sci 19(2):203–215
15. Da Silva WRL, Štemberk P (2012) Predicting self-compacting concrete shrinkage based on a modified fuzzy logic model. Eng Mech 229:1173–1183
16. Da Silva WRL, Štemberk P (2013) Expert system applied for classifying self-compacting concrete surface finish. Adv Eng Softw 64:47–61
17. Nehdi ML, Bassuoni MT (2009) Fuzzy logic approach for estimating durability of concrete. Proc ICE Constr Mater 162(2):81–92
18. Jin-li W, Hai-qing L (2010) Application of neural network in prediction for self-compaction concrete. Fuzzy information and engineering 2010. Springer, Berlin Heidelberg, pp 733–738
19. Uysal M, Tanyildizi H (2012) Estimation of compressive strength of self-compacting concrete containing polypropylene fiber and mineral additives exposed to high temperature using artificial neural network. Constr Build Mater 27(1):404–414
20. Siddique R, Aggarwal P, Aggarwal Y (2011) Prediction of compressive strength of self-compacting concrete containing bottom ash using artificial neural networks. Adv Eng Softw 42(10):780–786
21. Güneyisi E, Gesoglu M, Özbay E (2009) Evaluating and forecasting the initial and final setting times of self-compacting concretes containing mineral admixtures by neural network. Mater Struct 42(4):469–484
22. Zhou S, Shi J, Yang X, Lei L (2005) Application of neural network in prediction for flowing property of self-compacting concrete. J Water Resour Archit Eng 4:012

23. Li FX, Yu QJ, Wei JX, Li JX (2011) Predicting the workability of self-compacting concrete using artificial neural network. Adv Mater Res 168:1730–1734
24. Prasad BK, Eskandari H, Reddy BV (2009) Prediction of compressive strength of SCC and HPC with high volume fly ash using ANN. Constr Build Mater 23(1):117–128
25. Lippmann RP (1987) An introduction to computing with neural nets. ASSP Mag IEEE 4(2):4–22
26. Rumellhert D, Hinto G, Williams R (1986) Learning internal representations by error propagation. MIT Press, Cambridge
27. Dhiyaneshwaran S, Ramanathan P, Baskar I, Venkatasubramani R (2013) Study on durability characteristics of self-compacting concrete with fly ash. Jordan J Civ Eng 7(3):342–352
28. Bingöl AF, Tohumcu İ (2013) Effects of different curing regimes on the compressive strength properties of self compacting concrete incorporating fly ash and silica fume. Mater Des 51:12–18
29. Gettu R, Izquierdo J, Gomes PCC, Josa A (2002) Development of high-strength self-compacting concrete with fly ash: a four-step experimental methodology. In: Proceedings of the 27th conference on our world in concrete and structures, Paramasivam y TH Tan, Singapore, pp 217–224
30. Güneyisi E, Gesoğlu M, Özbay E (2010) Strength and drying shrinkage properties of self-compacting concretes incorporating multi-system blended mineral admixtures. Constr Build Mater 24(10):1878–1887
31. Krishnapal P, Yadav RK, Rajeev C (2013) Strength characteristics of self compacting concrete containing fly ash. Res J Eng Sci ISSN 2278:9472
32. Mahalingam B, Nagamani K (2011) Effect of processed fly ash on fresh and hardened properties of self compacting concrete. Int J Earth Sci Eng 4(5):930–940, ISSN 0974-5904
33. Muthupriya P, Sri PN, Ramanathan MP, Venkatasubramani R (2012) Strength and workability character of self compacting concrete with GGBFS, FA and SF. Int J Emerg Trends Eng Dev 2(2):424–434, ISSN 2249-6149
34. Nepomuceno MC, Pereira-de-Oliveira LA, Lopes SMR (2014) Methodology for the mix design of self-compacting concrete using different mineral additions in binary blends of powders. Constr Build Mater 64:82–94
35. Patel R (2003) Development of statistical models to simulate and optimize self-consolidating concrete mixes incorporating high volume of fly ash. Dissertation, University of Ryerson, Toronto
36. Şahmaran M, Yaman İÖ, Tokyay M (2009) Transport and mechanical properties of self consolidating concrete with high volume fly ash. Cem Concr Compos 31(2):99–106
37. Siddique R (2011) Properties of self-compacting concrete containing class F fly ash. Mater Des 32(3):1501–1507
38. Siddique R, Aggarwal P, Aggarwal Y (2012) Influence of water/powder ratio on strength properties of self-compacting concrete containing coal fly ash and bottom ash. Constr Build Mater 29:73–81
39. Uysal M, Yilmaz K (2011) Effect of mineral admixtures on properties of self-compacting concrete. Cem Concr Compos 33(7):771–776
40. Demuth H, Beale M, Hagan M (2007) Neural network toolbox 5, user's guide. The MathWorks Inc, Natick, p 849
41. Zhu W, Bartos PJ (2003) Permeation properties of self-compacting concrete. Cem Concr Res 33(6):921–926
42. Naik TR, Kumar R, Ramme BW, Canpolat F (2012) Development of high-strength, economical self-consolidating concrete. Constr Build Mater 30:463–469
43. Turk K, Karatas M, Gonen T (2013) Effect of fly ash and silica fume on compressive strength, sorptivity and carbonation of SCC. KSCE J Civ Eng 17(1):202–209
44. Liu M (2010) Self-compacting concrete with different levels of pulverized fuel ash. Constr Build Mater 24(7):1245–1252
45. Yen T, Tang CW, Chang CS, Chen KH (1999) Flow behavior of high strength high performance concrete. Cem Concr Compos 21(5):413–424
46. Aïtcin PC (1994) The use of superplasticizers in high performance concrete. In: Malier Y (ed) High performance concrete: from material to structure. E & FN Spon, London, pp 14–33